

## Study of Zircon Crystals: An Implication to Determine of Source and Temperature of Crystallization in Turkeh Dareh Pluton, NW Iran

M. Jamshidibadr\*

*Department of Geology, Faculty of Sciences, University of Payam Noor, Tehran, Islamic Republic of Iran*

Received: 23 May 2016 / Revised: 23 June 2016 / Accepted: 10 August 2016

### Abstract

Turkeh Dareh pluton is outcrop in NW of Iran and it is one of the intrusions in Sanandaj-Sirjan zone. Shaped crystals of this pluton distinct oscillatory zoning narrow and close together zoning in zircons indicate parental magma richness of zirconium. Factors affecting the shape of the zircon crystals are the composition, possibly the temperature of the crystallization, water content in magma and origin of the magma, therefore, were studied morphology of zircon crystals of Turkeh Dareh pluton. Morphologically, most of Turkeh Dareh zircons are located in range of S13 and S14 and in lesser extent in the range of S18, S19 and S20. The minimum zircons crystallization temperature was calculated 750 to 840 C° based on the morphology of zircon, zircon saturation and the whole rock geochemistry. The origin of intrusion magma of Turkeh Dareh is I-type and calc-alkaline that these results are consistent with results of field observations, mineralogy and geochemistry of this pluton.

**Keywords:** Morphology of zircon; Thermometer; Turkeh Dareh Pluton; Sanandaj-Sirjan zone; Iran.

### Introduction

The resistance of zircon to chemical and mechanical processes as well as its high melting point is so high that it can remain intact and unchanged within the earth crust for millions of years, and therefore it can survive from processes such as weathering, transportation, high temperature metamorphism and even partial melting. Morphology of zircons is closely related to the origin, development, and chemical composition and geological position of its parental magma [1-14]. Zircon crystallizes in the tetrahedral system in the form of two-way prismatic crystals with length to width ratio of one

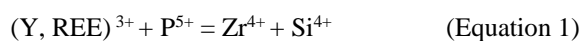
to five. The high ratio of length to width in this mineral is signs of rapid crystallization of parental magma [15].

In addition, zircon has great tendency to trace elements, which are distributed in different zones representing changes in elements during magmatic evolution [16]. Pupin [2] ranked zircon crystals based on relative growth of prismatic shapes {100} to {110} and pyramidal {211} to {101}. Pupin [2] suggested that the zircon typology is a function of chemistry and crystallization temperature of a magma from which zircon crystallizes. He further shown that the relative growth of pyramidal shapes with a chemical composition (ratio Al / (Na + K) or indexes A and

\* Corresponding author: Tel: +982645383686; Fax: +982645383244; Email: m\_jamshidi@pnu.ac.ir

relative growth of pyramidal shapes are directly related to the crystallization temperature. In other words, zircons crystallized from aluminous liquids have pyramids {211} and zircons crystallized in the {101} in alkaline conditions have pyramid with developed levels. According to Pupin [2], magma temperature is the most important factor controlling relative growth of various prismatic shapes in zircon crystals. Therefore, crystallized shape of zircon can be used as thermometer.

However, as Vavra [17] interpreted growth rate and size of zircon crystals are controlled oversaturation of melt from  $\text{ZrSiO}_4$  and the amount of trace elements and these factors are more important than temperature. According to him, pyramids morphology (eg {211} versus {101}) is basically controlled external trace elements, while the prism form is determined the supersaturation degree of  $\text{ZrSiO}_4$ . According Benisek & Finger [16], the amount of uranium and equation 1 are important factor of growth in prisms {110} of zircon. That is why the granitic magmas containing low levels of U, Th, Y, REE and P (compared to Zr) crystallize zircons with large prisms {100}.



Investigation morphology of zircon crystals in granite rocks, primary magma source was introduced different researchers for e.g [2, 18, 19]. They distinguished magma sources of three groups of granites-I (tholeiitic and alkaline granite high temperature), granites-S (moderate temperature granites derived from shells or aluminous) and two-vein granites (low temperature granites of calcic-alkaline and sub-alkaline series).

In this study, zircon was used to investigate the origin of the magma and parental magma thermometer of Turkeh Dareh pluton, due to its specific characteristics such as chemical and mechanical characteristics and high melting point. Turkeh Dareh intrusion has outcrop in the North West of Iran and among cities of Shahindej and Takab and it is among the intrusions of Sanandaj-Sirjan zone introduced in the geological map of 1:100,000 in Shahin Dej [20] and Chapan [21] (Fig. 1). The age of Turkeh Dareh intrusion is  $59.0 \pm 2.7$  based on U-Pb dating of zircon reported by [22] and the age of regional metamorphism (schist) were dated from a garnet-schist using the yielded a  $^{238}\text{U}/^{206}\text{Pb}$  age of monazites  $61 \pm 8$  ma that reported by [23]. Using morphology of zircon separated from intrusion rocks of Turkeh Dareh and field features,

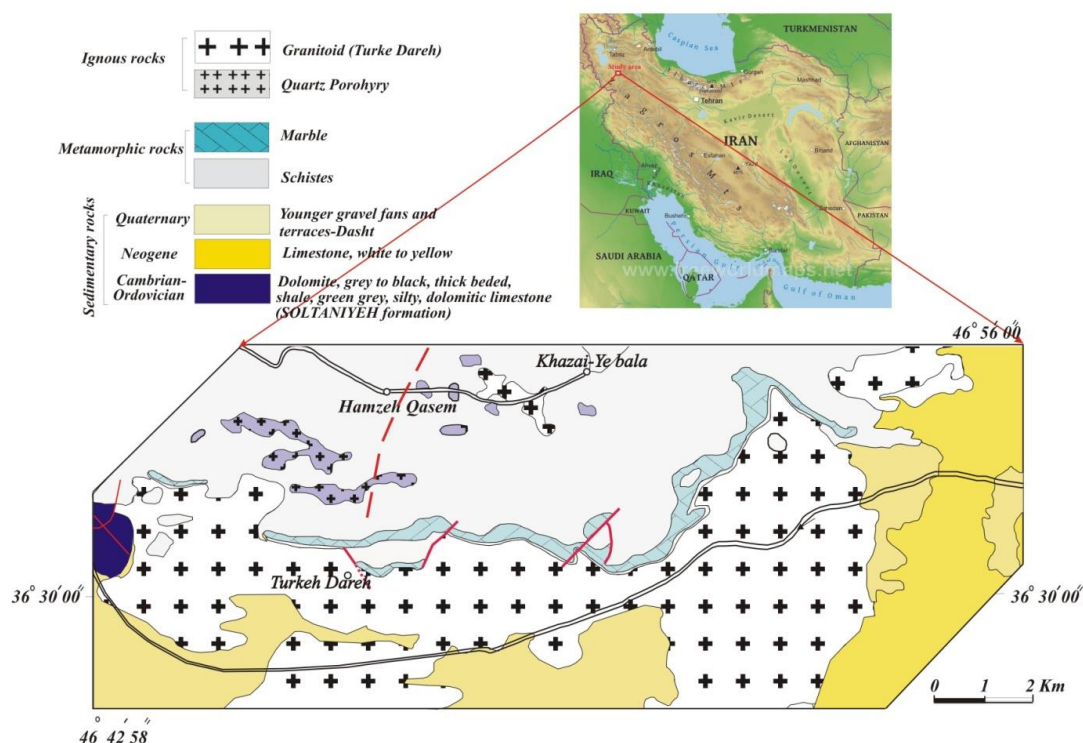


**Figure 1.** A) Location of Turkeh Dareh Pluton Shown in the Iran map, B) Turkeh Dareh granitoids shown in simplified Geological Map of Shahin Dezh from [19] and Chapan from [20] scale of 1:100000.

geochemistry and geomorphology of this pluton was discussed so that the relationship between these studies can be a model for future studies. The study of zircon morphology used only for igneous zircons, its not be used for metamorphic zircons [2, 18, 19].

### Materials and Methods

The zircon separation was carried out in the laboratories of the University of Adelaide in Australia.

Zircons were separated using conventional methods that include crushing, sieving, magnetic separation and floatation. More than fifty zircon grains were handpicked under a binocular microscope. The zircons were then set in synthetic resin mounts, polished and cleaned in a warm  $\text{HNO}_3$  ultrasonic bath. Cathodoluminescence (CL) and back-scattered electron (BSE) imaging were carried out to help characterize any

compositional variation within individual zircons (Figs. 2 & 3). After microscopic studies, 8 samples were selected for whole rock geochemistry studies. Analysis was conducted using XRF method in Tehran Tarbiat Moallem (teacher training) University (Table 1).

### General geology

Turkeh Dareh pluton has light to dark gray color (Figs. 4a & b) and in some parts centralization of minerals in one part and dark minerals in other part caused layer in this mass leading to light and dark gray in this part (Fig. 4c). Due to centralization of dark minerals in some parts of different samples with different colors to differentiate the zircon and petrographic and geochemical studies, sample was taken and examined. In microscopic studies, this pluton had granular texture and in terms of mineralogy it has euhedral to subhedral plagioclase with polysynthetic

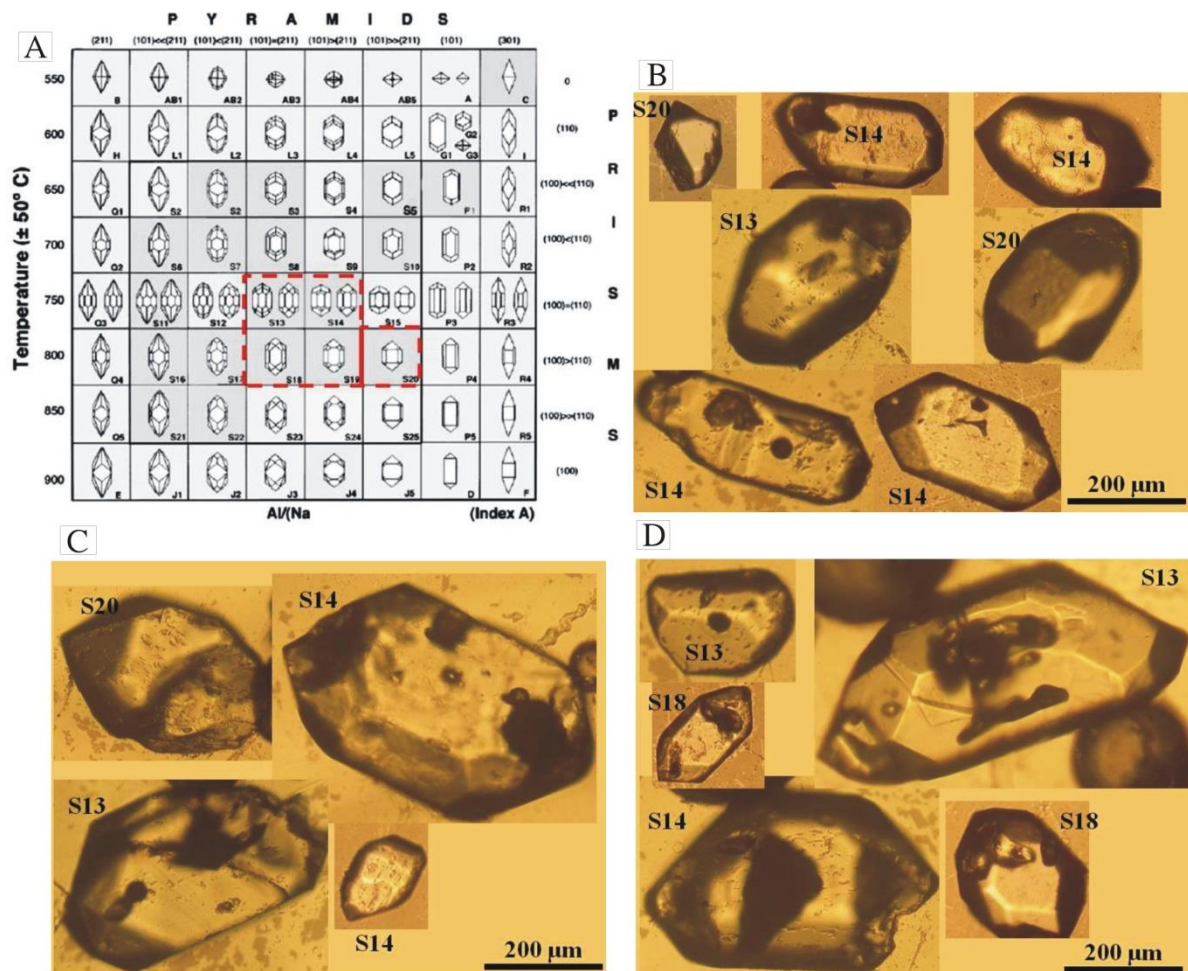


**Figure 2.** A) The location of various types of zircon crystals within petrogenetic categorization of Pupin [2], B), C) and D) Zircon crystals of Turkeh Dareh pluton and their classification based on morphology after [2].

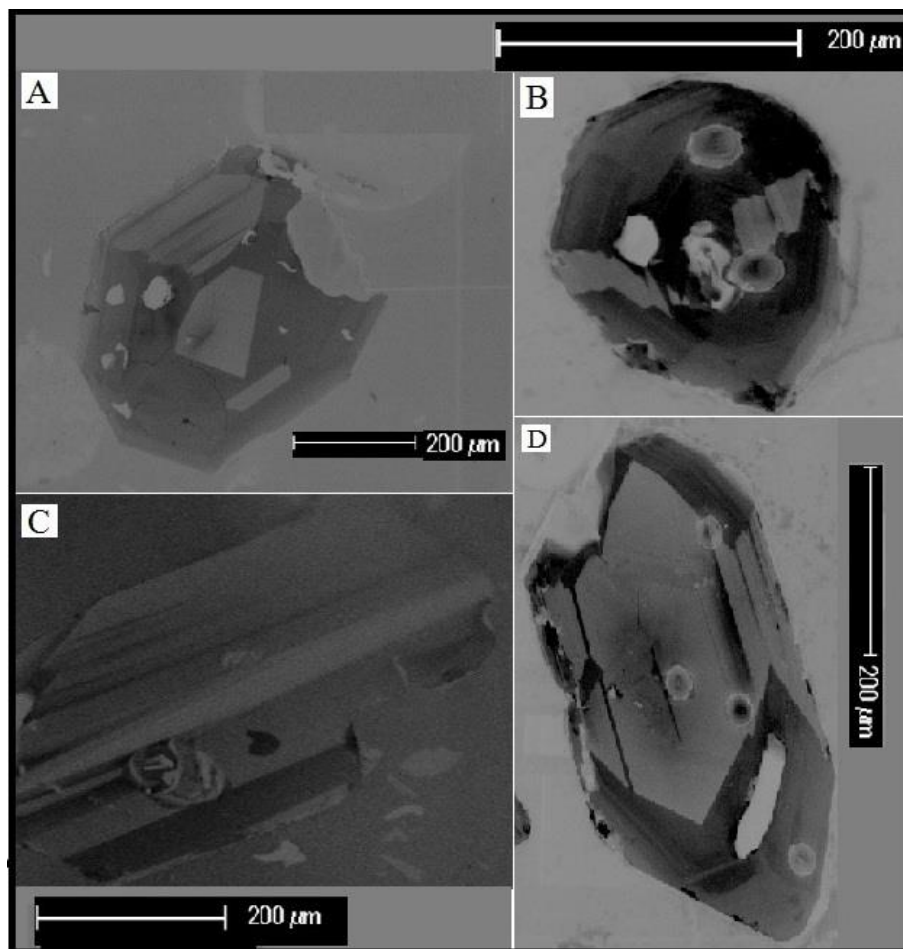


**Figure 3.** A), B), C) and D) Cathodoluminescence images of zircon grains showing long, euhedral and oscillatory zoning (the scale bar is 200 µm)[21].

**Table 1.** XRF analyses on Turkeh Dareh granitoids [21] and calculation of M, degree of saturation and saturation temperature of zircon

Samples	SiO <sub>2</sub>	Al <sub>2</sub> O <sub>3</sub>	CaO	Na <sub>2</sub> O	K <sub>2</sub> O	TiO <sub>2</sub>	Zr	M	T °C watson and harrison (1983)	T °C watson and harrison [6] calculated	T °C Boehnke et al. [7] calculated
T-108	70.73	13.87	3.15	3.34	2.83	0.4	324	1.51	787.70	841.13	800.36
T-181	68.98	13.53	3.64	5.8	2.09	0.35	338	2.07	787.70	801.32	735.97
T-186	65.7	14.82	3.41	4.56	3.43	0.68	367	1.86	787.70	825.07	769.75
T-325	67.58	13.74	3.73	4.66	3.45	0.69	344	2.05	787.70	803.79	739.12
T-109	72.64	13.12	2.09	4.85	3.59	0.15	292	1.73	787.70	814.03	761.26
T-182	64.21	12.71	4.54	4.78	3.04	0.88	376	2.43	787.70	783.81	705.66
T-184	62.73	15.68	4.18	4.5	3.02	0.84	374	1.91	787.70	822.44	764.88
T-183B	62.51	12.1	4.26	4.76	3.02	0.91	386	2.48	787.70	782.32	702.53

twinning, anhedral quartz, and alkali feldspar and mafic minerals in the pluton are biotite and amphibole. The accessory minerals of this pluton include titanite that are perfectly shaped and dark brown color, zircon and apatite (Figs. 5a, b & c). From mineralogy perspective, dark and light parts of this pluton are not different and

only modal percentage of felsic and mafic minerals in this parts is different. Light parts have high frequency of felsic minerals than mafic minerals. In naming Streckeisen & LeMaitre [24], modal of this pluton can be seen in the range of granodiorite and monzodiorite (Fig. 6a).



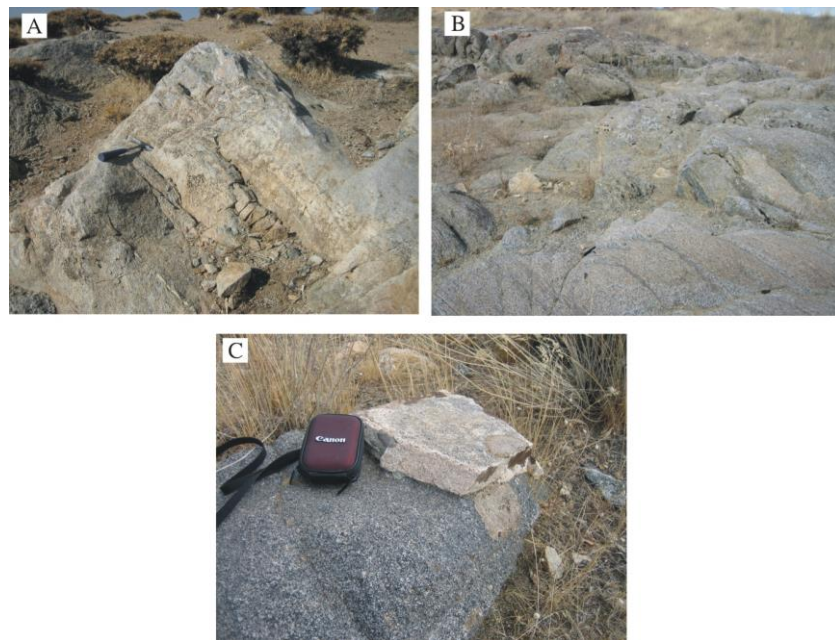


**Figure 4.** Turkeh Dareh pluton outcrop. A) Light gray color including quartz, plagioclase, K-feldspar, and some amphibole and biotite, B) magmatic banding from Turkeh Dareh pluton, C) centralization of hornblende and biotite in some parts of Turkeh Dareh pluton that shows dark gray color.

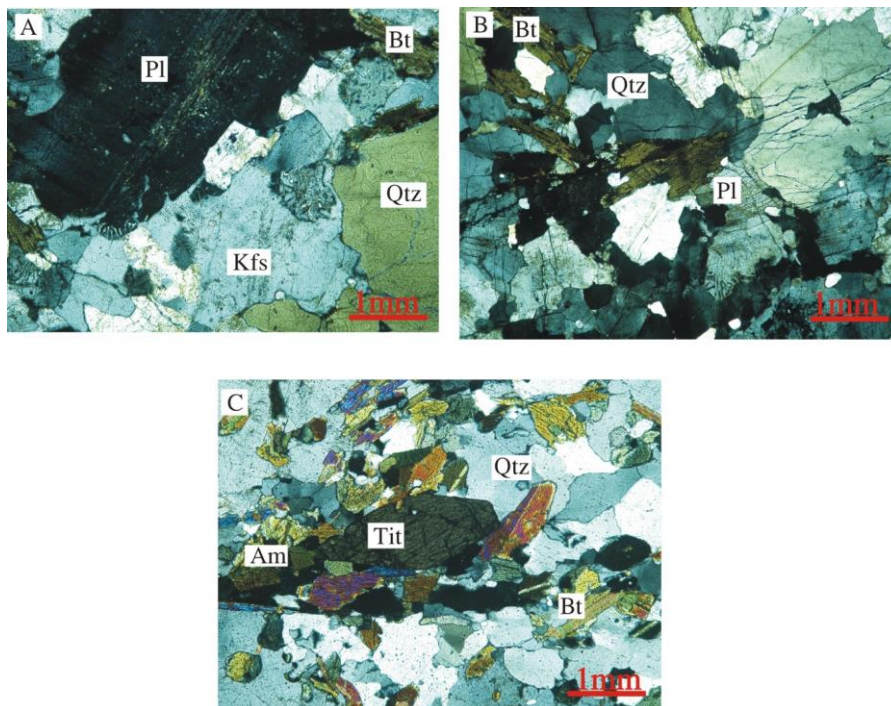


**Figure 5.** A) microphotograph from a light gray area of Turkeh Dare pluton granitoids. Felsic minerals are more abundant than (B) microphotograph. myrmekitic texture seen in centre of photo, C) microphotograph of dark band from Turkeh Dare pluton granitoids. The rock contains quartz, plagioclase, K-feldspar, hornblende, biotite, Titanite. Note that the hornblende and biotite are oriented.

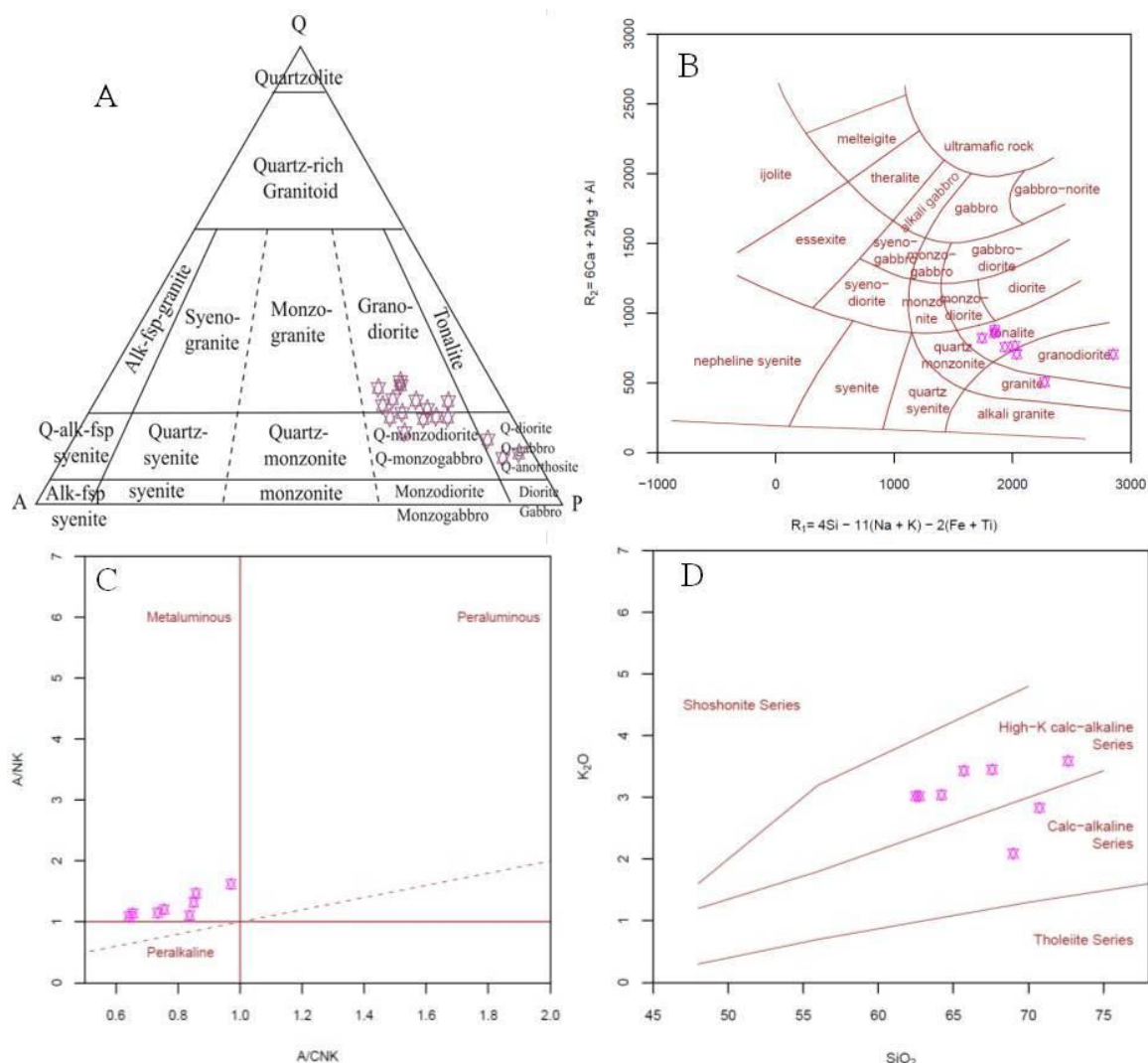


**Figure 6.** A) Modal classification of Streckeisen & LeMaitre [23] for Turkish Dareh granitoid rocks, B) The classification of Turkish Dareh pluton using the parameters  $R_1$  and  $R_2$  after [24], calculation from millication proportions.  $R_1 = 4Si - 11(Na + K) - 2(Fe + Ti)$ ;  $R_2 = 6Ca + 2Mg + Al$ , C) Shand's molar parameters  $A/NK = Al_2O_3 / (Na_2O + K_2O)$  vs  $A/CNK = Al_2O_3 / (CaO + Na_2O + K_2O)$  after [26]. D)  $K_2O$ - $SiO_2$  diagram illustrating the calc-alkaline and high-K calc-alkaline affinities of the Turkish Dareh granitoids [21].

## Results

### Whole rock geochemistry

According to field and petrographic studies Turkish Dareh pluton have dark and light parts in which  $Na_2O$ ,  $K_2O$ , and  $SiO_2$  frequency in light parts is greater than dark parts due to centralization of felsic minerals in light parts, and frequency percentage of  $Fe_2O_3$ ,  $MgO$ , and  $CaO$  in samples related to dark parts is higher than light parts (table 1). In the multi-cationic  $R_1$ - $R_2$  diagram [25] samples of Turkish Dareh are mainly in the range of granodiorite and tonalite (Fig. 6b). Regarding saturation of aluminum [26] samples of Turkish Dareh intrusions

have vales of  $A/CNK < 1.1$ , and they are in the range of I-type granites and magmatic series of Turkish Dare calc-alkaline with high and moderate potassium (Figs. 6c & d). Turkish Dareh pluton have weak anomaly ( $Eu/Eu^* = 0.95-1.48$ ) related to absence or slight subtract of plagioclase. The negative anomalies in Nb and Ta in normalized graphs can indicate that their formation is in subduction zones that is result of fluids and melts due to subducted lithospheric with metasomatism of mantle wedge above themselves [28]. In the tectonic environment separation diagrams, Turkish Dareh pluton samples are in the range of volcanic arc [22].

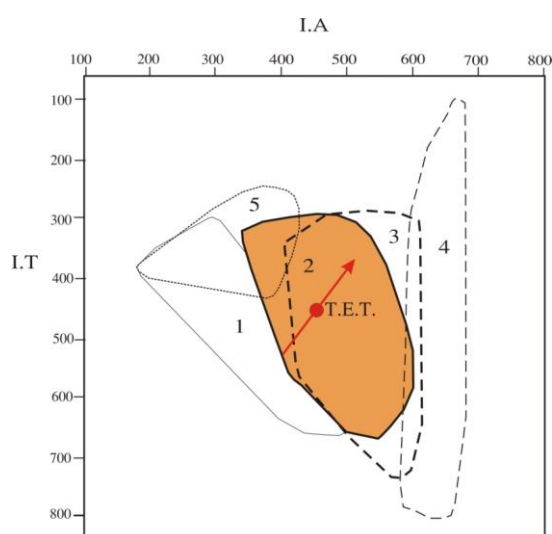


**Figure 7.** The crossing point of I.T and I.A and the value of T.E.T calculated for zircons of the studied area and the position of this trend on Pupin [2] diagram, distribution of plutonic rocks in the typologic diagram: (1) diorites, quartz, gabbros and diorites; (2) granodiorites; (3) monzogranites and monzonites; (4) alkaline and hyperalkaline syenites and granites; (5) cordierite bearing rocks.

### Morphology of zircon crystals

Zircon crystals separation of various samples of Turkeh Dareh intrusion that had different frequency in mafic and felsic minerals was conducted. Separated zircons are honey yellow to colorless and transparent to translucent with zoning. In terms of morphology, most of zircon crystals in the classification of Pupin [2] are in the range of S14 and S13 and to a lesser extent in the range of S18, S19 and S20 (Figs. 2, 3 & 7). With regard to the distribution of zircons in the diagram provided from Pupin [2], the mean values of Alkalinity Index (IA) and Temperature Index (IT) that were calculated distribution of studied zircons in the diagram of Pupin [2] are respectively 461.8 and 445.5 (Tables 2a & b). In

addition, to calculate typological evolutionary trend, a line with slope of  $ST/SA$  (standard of deviation of index T/and standard deviation of index A) has been drawn from intersection of I.A and I.T that is equals to tangent of angle of two axes T.E.T and I.A [2]. The typological evolutionary trend measured for studied zircons has angle of 46.02 degrees with axis I.A. Therefore, values I.A, I.T zircon typological trend of studied granitoids are similar to zircons with calc-alkaline magmatic origin and they are at the range of granodiorite, monzonite, and monzogranites (Fig. 7).

## Discussion

### Geo-thermometry of crystals of zircon

Based on crystals of zircon [2] and equations provided from [6, 7] and using geochemical data, we can estimate the minimum temperature of zircon formation in a magmatic source. Using the above-mentioned cases, minimum temperature of Turkeh Dareh intrusion rocks was calculated.

### Geo-thermometry of Turkeh Dareh pluton based on crystal shapes of zircon

Based on the morphology of zircon crystal, zircon crystallization temperature of Turkeh Dareh pluton was determined about 750 to 800 ° C (Fig. 7) (Tables 2a & b).

### Geo-thermometry of Turkeh Dareh pluton based on zircon saturation

To determine the minimum temperature of zircon crystallization using saturation temperature [6, 7, 29, 30, 31, 32], specified conditions from Janousek & Saturnin [29] must exist in intrusion. The necessary conditions are that magma nature must be meta-aluminous, the absence of inherited zircons, zircon uniform distribution in entire rock and negative correlation between elements

**Table 2.** A) Morphological frequency distribution of zircon crystals on the basis of quantity and frequency of occurrence in Turkeh Dareh intrusion, B) zircon crystals emplacement within the area of 750 to 800°C° on Pupin [2] diagram.

A)			T°C	B)								
Shapes	Quantity	%		Al/(K+Na)								
S13	16	44.4		100	200	300	400	500	600	700	800	
S14	14	38.9		550	0	0	0	0	0	0	0	0
S18	9	25.0		600	0	0	0	0	0	0	0	0
S19	12	33.3		650	0	0	0	0	0	0	0	0
S20	4	11.1		700	0	0	0	0	0	0	0	0
Total	55	100		750	0	0	0	16	14	0	0	0
				800	0	0	0	9	12	4	0	0
				850	0	0	0	0	0	0	0	0
				900-	0	0	0	0	0	0	0	0
				1200								

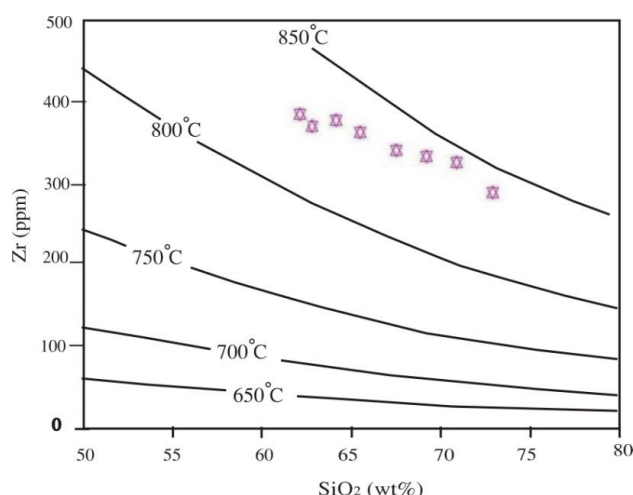


**Figure 8.** Zr vs. SiO<sub>2</sub> diagram from [6] for determination of crystallization temperature of Turkeh Dareh granitoids

of zirconium and silica that these correlations are also true in the Turkeh Dareh pluton.

#### **Calculation of temperature based on Zircon saturation using Watson and Harrison Equation**

Watson and Harrison [6] confirmed the relationship between the solubility of zircon, temperature, and composition of the melt based on Equation 2:

$$\ln D_{Zr} = \{12900/T (K)\} - 0.85 (M-1) - 3.80 \quad (\text{Equation 2})$$

In this equation,  $\ln D_{Zr}$  is rate of zirconium concentration in zircon (500000 ppm) relative to the concentration of zirconium in molten (ppm).  $T$  represents the temperature in Kelvin and  $M$  is a cationic ratio depending on SiO<sub>2</sub> and aluminous melt calculated through Equation 3:

$$M = [(Na + K + 2Ca)/(Al.Si)] \quad (\text{Equation 3})$$

According to Equation provided after Watson and Harrison [6], zircon crystallization temperature of Turkeh Dareh intrusion was calculated 782 to 825 C° (Table 1).

Calculation of temperature based zircon saturation using Equation of Boehnke et al [7] revised the relationship between the solubility of zircon, temperature and composition of the molten provided from Watson and Harrison [6] and provided Equation 4 to estimate the saturation temperature of zircon (variables are like Equation 2):

$$\ln D_{Zr} = \{(10108 \pm 32)/T (K)\} - (1.16 \pm 0.15) (M-1)$$

$$- (1.48 \pm 0.09) \quad (\text{Equation 4})$$

According to equation Boehnke et al [7], zircon crystallization temperature of Turkeh Dareh intrusion was calculated 702 to 800 C° (Table 1). According to the graph Zr versus SiO<sub>2</sub> of Watson and Harrison [6], the minimum crystallization temperature of Turkeh Dareh intrusion is 820 to 845 C° (Fig. 8).

To determine origin of Turkeh Dareh intrusion on the basis of the morphology of zircon, graph of Gehmich & Drost [18] was used. In this method, due to morphology of Turkeh Dareh intrusion zircons that are in the ranges of IIa, IIb, IIc, the magma origin of Turkeh Dareh intrusion is calc-alkaline and I-type (Fig. 9).

Observing distinct oscillatory zoning, typical of magmatic crystallization in Turkeh Dareh intrusion zircon indicate supersaturation of magma compared to zirconium from beginning of crystallization to final stages. The minimum zircon crystallization temperature in granitoides studies based on morphology is 700 to 850 C° 0, based on zircon saturation temperature is 732 to 841 C° and based on whole rock geochemistry is 750 to 860 C°. Considering the results of thermometer and supersaturation of granitic magma from beginning of crystallization relative to zirconium and as zircon is among the first crystalized minerals, so temperature range of 750 to 840 C° can be considered as minimum temperature of magma crystallization Turkeh Dareh intrusion. Growth of pyramids {101} of most zircons in the Turkeh Dareh intrusion represents origin of their calc-alkaline that it is consistent with the results of whole rock chemistry. Growth of prisms {100} in these zircons represents its high temperature index confirmed results of geothermometry. Based on mineralogy,



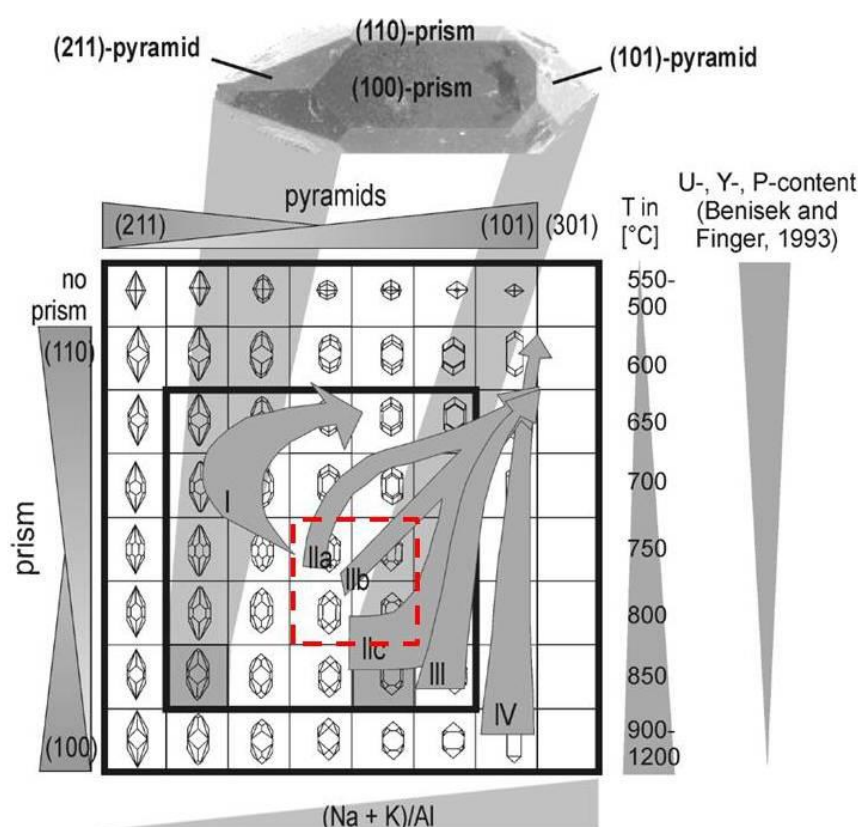


**Figure 9.** Pupin scheme showing the zircon morphology depending on  $(\text{Na} + \text{K})/\text{Al}$ , and formation temperature [2] or on the content of U, Y, and P [7] with different trends: Legend: I = Al-rich anatectic granitoids; IIa,b,c = calc-alkaline granitoids; III = K-rich subalkaline granitoids; IV = alkaline granitoids [18].

geochemistry, and morphology of zircon Turkeh Dareh intrusion is I-type granite.

### References

1. Salehi Z., Masoudi F., Razavi M. and Faramarzi N.S. Estimating of Crystallization Temperature of Mard-Abad (Karaj) Granitic Intrusion Using Mineralogy, Geochemistry and Morphology of Zircon Crystals. *J. Sci. I. R. Iran.* **25**(2): 143 - 155 (2014).
2. Pupin J.P. Zircon and granite petrology. *Contrib. Mineral. Petrol.* **73**: 207-220 (1980).
3. Gerdes A., Zeh A. Zircon formation versus zircon alteration – New insights from combined U–Pb and Lu–Hf in-situ LA-ICP-MS analyses, and consequences for the interpretation of Archean zircon from the Central Zone of the Limpopo Belt. *Chem. Geol.* **261** (3–4): 230–243 (2009).
4. Sturm R. Morphology and growth trends of accessory zircons from various granitoids of the south-western Bohemian Massif (Moldanubicum, Austria). *Chemie Erde.* **70**: 185–196 (2010).
5. Gagnevin D., Daly J.S., Kronz A. Zircon texture and chemical composition as a guide to magmatic processes and mixing in a granitic environment and coeval volcanic system. *Contrib. Mineral. Petrol.* **159**: 579–596 (2010).
6. Watson E.B. and Harrison T.M. Zircon saturation revisited: temperature and composition effects in a variety of crustal magma types. *Earth. Planet.* **64**:295-304 (1983).
7. Boehnke P., Watson E.B., Trail D., Harrison T.M. and Schmitt A.K. Zircon saturation re-revisited. *Chem. Geol.* **351**: 324-334 (2013).
8. Claiborne L.L., Miller C.F., Wooden J.L. Trace element composition of igneous zircon: a thermal and compositional record of the accumulation and evolution of a large silicic batholith, Spirit Mountain, Nevada. *Contrib. Mineral. Petrol.* **160**: 511–531 (2010).
9. Fu B., Mernagh T.P., Kita N.T., Kemp A.I.S., Valley J.W. Distinguishing magmatic zircon from hydrothermal zircon: a case study from the Gidginbung highsulphidation Au–Ag–(Cu) deposit, SE Australia. *Chem. Geol.* **259**: 131–142 (2009).
10. Grimes C.B., John B.E., Cheadle M.J., Mazdab F.K., Wooden J.L., Swapp S., Schwartz J.J. On the

- occurrence, trace element geochemistry, and crystallization history of zircon from in situ ocean lithosphere. *Contrib. Mineral. Petrol.* **158**: 757–783 (2009).
11. Shahbazia H., Salamia S., Wolfgang Siebel W. Genetic classification of magmatic rocks from the Alvand plutonic complex, Hamedan, western Iran, based on zircon crystal morphology. *Chem Erde-Geochem.* **74**(4): 577–584 (2014).
  12. Helena C., Brites Martins H.C., Simoes P.P., Abreu J. Zircon crystal morphology and internal structures as a tool for constraining magma sources: Examples from northern Portugal Variscan biotite-rich granite plutons. *C. R. Geoscience.* **346**: 233–243 (2014).
  13. Rustad J. Interaction of rhyolite melts with monazite, xenotime and zircon surfaces. *Contrib. Mineral. Petrol.* **169**: 50–58 (2015).
  14. Bindeman L.N. and Melnik O.E. Zircon Survival, Rebirth and Recycling during Crustal Melting, Magma Crystallization, and Mixing Based on Numerical Modelling. *J. Petrol.* **57**(3): 437–460 (2016).
  15. Belousova E.A., Griffin W.L., O'Reilly S.Y. and Fisher N.J. Igneous zircon: trace element composition as an indicator of source rock type. *Contrib. Mineral. Petrol.* **143**: 602–622 (2002).
  16. Benisek A. and Finger F. Factors controlling the development of prism faces in granite zircons: a microprobe study. *Contrib. Mineral. Petrol.* **114**: 441–451 (1993).
  17. Vavra G. On the kinematics of zircon growth and its petrogenetic significance: A cathodoluminescence study. *Contrib. Mineral. Petrol.* **106**: 90–99 (1990).
  18. Gehmlich M. and Drost K. Cadomian and Early Paleozoic magmatic events: Insights from zircon morphology and geochemical signatures of I- and S-Type granitoids (Saxo-Thuringia/Bohemian Massif/Central Europe). *Int. Geol. Rev.* **47**: 1287–1297 (2005).
  19. Rottura A., Bargossi G. M., Caironi V., D'Amico C. and Maccarone E. Petrology and geochemistry of late Hercynian granites from the Western Central System of the Iberian Massif. *Eur. J. Mineral.* **1**: 667–683 (1989).
  20. Kholghi Khasraghi M.H. Quadrangle Geological Map of Shahin Dezh, Scale 1:100000. *Geol. Surv. Iran* (1994).
  21. Kholghi Khasraghi M.H. Quadrangle Geological Map of Chapan, Scale 1:100000. *Geol. Surv. Iran* (1994).
  22. Jamshidi Badr M., Masoudi F., Collins A.S. and Cox C. The UPb Age, Geochemistry and Tectonic Significance of Granitoids in the Soursat Complex, Northwest Iran. *Turk. J. Earth. Sci.* **22**: 1–31 (2013).
  23. Jamshidi Badr M., Masoudi F., Collins A.S. and Cox C. Dating of Precambrian Metasedimentary Rocks and Timing of their Metamorphism in the Soursat Metamorphic Complex (NW IRAN): Using LA-ICPMS, U–Pb Dating of Zircon and Monazite. *J. Sci. I. R. Iran.* **21**(4): 311–319 (2010).
  24. Streckeisen A. and Le Maitre R.W. A Chemical Approximation to the Modal QAPF Classification of the Igneous Rocks. *Neu. Jb. Mineral. Abh.* **136**: 169–206 (1979).
  25. De La Roche H., Leterrier J., Grandclaude P. and Marchal M. A classification of volcanic and plutonic rocks using R1-R2 diagram and major element analyses: its relationships with current nomenclature. *Chem. Geol.* **29**: 183–210 (1980).
  26. Chappell B.W. and White A.J.R. I- and S-type granites in the Lachlan fold belt. Transactions of the Royal Society of Edinburgh. *Earth. Sci.* **83**: 1–26 (1992).
  27. Maniar P.D. and Piccoli P.M. Tectonic discrimination of granitoids. *Geol. Soc. Am. Bul.* **101**: 635–643 (1989).
  28. Chappell B.W. Aluminium saturation in I- and S-type granites and the characterization of fractionated haplogranites. *Litho.* **46**: 535–551 (1999).
  29. Janousek V. and Saturnin R. Language script for application of accessory-mineral saturation models in igneous geochemistry. *Geol. Carpath.* **57**: 131–142 (2006).
  30. Harrison T.M., Watson E.B. and Aikman A.B. Temperature spectra of zircon crystallization in plutonic rocks. *Geol.* **35**(7): 635–638 (2016).
  31. Fernanda Gervasoni F., Klemme S., Rocha-Júnior E.R.V. and Berndt J. Zircon saturation in silicate melts: a new and improved model for aluminous and alkaline melts. *Contrib. Mineral. Petrol.* **171**: 1–21 (2016).
  32. Hengzhong Qiao H., Yin C., Li Q., Xiaolan He X., Qian J. and Li W. Application of the revised Ti-in-zircon thermometer and SIMS zircon U–Pb dating of high-pressure pelitic granulites from the Qianlishan-Helanshan Complex of the Khondalite Belt, North China Craton. *Precambrian Res.* **276**: 1–13 (2016).